Measurements Selection for Bias Reduction in Structural Damage Identification

Yuhang Liu
Department of Industrial and Systems Engineering,
University of Wisconsin-Madison, Madison,
3255 Mechanical Engineering,
1513 University Ave
Madison, WI 53706, USA
Email: liu427@wisc.edu

Shiyu Zhou¹
Department of Industrial and Systems Engineering, University of Wisconsin-Madison, Madison, 1513 University Ave Madison, WI 53706, USA Email: shiyuzhou@wisc.edu

Yong Chen
Department of Mechanical and Industrial Engineering
University of Iowa, Iowa City,
IA 52242, USA
Email: yong-chen@uiowa.edu

Jiong Tang
Department of Mechanical Engineering,
University of Connecticut, Storrs,
Storrs, CT 06269, USA
Email: jtang@engr.uconn.edu

Abstract Linearization of the eigenvalue problem has been widely used in vibration-based damage detection utilizing the change of natural frequencies. However, the linearization method introduces bias in the estimation of damage parameters. Moreover, the commonly employed regularization method may render the estimation different from the true underlying solution. These issues may cause wrong estimation in the damage severities and even wrong damage locations. Limited work has been done to address these issues. It is found that particular combinations of natural frequencies will result in less biased estimation using linearization approach. In this paper, we propose a measurement selection algorithm to select an optimal set of natural frequencies for vibration-based damage identification. The proposed algorithm adopts L_1 - norm regularization with iterative matrix randomization for estimation of damage parameters. The selection is based on the estimated bias using the least square method. Comprehensive case analyses are conducted to validate the effectiveness of the method.

Keywords: Structural damage identification, Bias reduction, Compressed sensing, L_1 -norm minimization, Natural frequencies

¹ Corresponding author

NOTATION	
M	global mass matrix
K	global stiffness matrix
$\mathbf{K}^{\mathbf{d}}$	global stiffness matrix for damaged structure
$\mathbf{K}_{j}^{(\mathrm{e})}$	the jth elemental stiffness matrix
$\mathbf{x}(t)$	nodal displacements
$\mathbf{F}(t)$	nodal forces
f_i	the <i>i</i> th natural frequencies
$\mathbf{\phi_i}$	the <i>i</i> th mode shape
λ_i	the <i>i</i> th eigenvalue, $\lambda_i = f_i^2$
$\boldsymbol{\varphi_{i}^{\mathit{d}}}$	the ith mode shape for damaged structure
λ_i^d	the ith eigenvalue for damaged structure
\Deltalpha_j	the percentage of stiffness change of the jth element
$\Delta oldsymbol{lpha}^{ m truth}$	the underlying truth of stiffness loss
$\widehat{\Delta oldsymbol{lpha}}$	the estimation of $\Delta \alpha^{\text{truth}}$
S	the first order of sensitivity matrix
$\mathbf{S^{(k)}}$	the subset of S , only contains rows that in the k th combination of natural
$\mathbf{c}(k)$	frequencies
$\underline{\mathbf{S}}^{(k)}$	the subset of $S^{(k)}$, only contains columns that elements are estimated as
	damaged
e	the error in the linearization $\Delta \lambda = S \Delta \alpha$
Φ (-)	the random Gaussian matrix
$\mathbf{L}^{(q)}$	the location of estimated non-damage element at qth iteration

1. Introduction

The timely and accurate identification of damage conditions in structures using real-time, online sensor measurements plays a critical role in ensuring the secure and sustainable operations of various structural systems in aerospace, marine, transportation and infrastructure, and energy and power industries. Among different structural damage identification techniques, the vibration-based methods [1] have been widely used. The basic idea of vibration-based methods is that the structural properties (e.g., mass, stiffness, etc.) will change due to damages in structures and such changes will result in the change of vibration properties including natural frequencies [2], mode shapes [3] and their variants such as curvature [4], flexibility [5]. Typically, natural frequencies can be measured directly with high accuracy and thus are broadly used in practice [6].

In natural frequencies based damage detection methods, damages can be identified by solving the eigenvalue problem with linear approximation [7]. The linearization provides the simplicity and efficiency in the problem-solving process. With the linearization, the unknown parameters $\Delta \alpha$ can be estimated by the linear equation $\Delta \lambda = S\Delta \alpha$, where $\Delta \alpha$ is the change in structural properties, **S** is the first order sensitivity matrix and $\Delta \lambda$ is the difference of the eigenvalues (squared natural frequencies) between healthy and damaged structures. In practice, the measurements of natural frequencies involve noise and model updating [8,9] is often preferred to correct the model parameters in the finite element model (FEM) for an accurate estimation of $\Delta \alpha$.

However, there are generally two major challenges in damage identification based on the linearized relationship between $\Delta\lambda$ and $\Delta\alpha$. First, **S** is usually a wide rectangular matrix, i.e., the number of columns of **S** is much larger than the number of rows since the number of possible damaged elements are much larger than the number of available natural frequencies. Thus, the linear system is a highly underdetermined system. Second, the linear relationship is just an approximation of the true underlying relationship between $\Delta\lambda$ and $\Delta\alpha$. Thus, there will be bias in the solution obtained based on the linear relationship.

In the literatures, research works are available trying to address these two challenges in structural damage identification. To relieve the impact caused by the system underdetermination, one approach is to enlarge the number of the measurements in the system. Typically, natural frequencies are only guaranteed to be measured accurately for the lower order modes due to the limitation in both actuation and sensing. Thus, the number of available natural frequencies is often enlarged through physical modification of structures. For examples, a mass addition technique is explored in [2] to enrich the modal measurements. In this approach, the known masses are added to the structure and thus new modal data is achieved. Similar ideas on adding mass or stiffness to extract additional natural frequencies can be found in [3]. One disadvantage of this type of physical modification is the difficulty to implement in practice due to many physical restrictions. Another type of physical modification adopts piezoelectric transducers integration onto the structure. The integrated structure is an electro-mechanical system with tunable piezoelectric circuits. The tunable inductance can introduce additional natural frequencies. Examples on such type of electro-mechanical system can be found in [4]. The limitation of physical modification approach is that

the number of unknown possible damage elements is often still much larger than the available number of measurements.

Another approach addressing the underdetermination issue is to work with the underdetermined system directly and try to obtain a sparse solution. The rationale of this strategy is that structural faults typically occur only at a limited number of locations simultaneously. In [10], the authors propose a pre-screening strategy to address the underdetermination issue. The fault locations are ranked according to the likelihoods and the locations with low likelihoods are discarded in order to reduce the fault parameter space. There are two limitations of such approach. The first is the underlying assumption of the distribution in the likelihood function. The independent and identically distributed (i.i.d.) assumption of errors is not generally true in the structural damages. The simplification of the error terms may lead to unreliable ranking results. Also, the cut-off threshold in the ranking procedure is ad hoc and may vary in different systems. Another technique in obtaining the sparse solution is by regularization. For example, the adaptive Tikhonov regularization is adopted in [11] to improve the identification results with the measurement noise effects. Th linear matrix inequality methods are used to constrain the unknown stiffness parameters in [12]. Among different types of regularization, the L_1 norm of the solution is often added to the objective function as a penalty and it often returns solution with sparsity, i.e., estimates most of the unknown variables to be 0. L_1 regularization is the most commonly used penalty method in the structural damage identification. For example, the authors apply the L_1 norm on the number of the damage locations in [1]. The results are sparse with the true damage locations are recovered. However, it is found that applying L_1 regularization directly often cannot guarantee the solution quality in the sense of solution sparsity and consistency. Moreover, the bias induced by the linear approximation may further reduce the accuracy of damage estimation.

In the literature, discussions on the bias in damage estimation caused by the linearization error is limited. The linearization between the structural parameters and the system response is introduced in [13]. The higher order terms in the Taylor series expansion are ignored to achieve the simplification in the equation. However, there are no thorough discussions on how to address the bias issue, where such bias may lead to significant errors in damage identification. In available studies, adding nonlinear higher order terms has been proposed to reduce the impact of bias in the analysis [4, 14, 15]. For example, the equation $\Delta \lambda = S_1 \Delta \alpha + \Delta \alpha^T S_2 \Delta \alpha$ including both the first

and second order of perturbation incorporates the change of mode shapes, which enhances the accuracy of damage identification. However, such approach is not recommended in general due to the loss of the linear property in the equation, where the highly underdetermined nonlinear system becomes the new challenge. Also, the improvements in the solution quality may not be worth the loss of the simplicity and the efficiency in the solution process. In recent studies of structural damage identification, applying deep neural network (DNN) to the problem becomes a new trend [16]. DNN generates reasonable results with high quality training data and well-designed network structures, e.g., the choice of activation functions and the layer of the network. It is expected that the bias can be reduced by applying multiple layers of linear functions. However, the DNN is a black box approach and may be ad hoc when selecting the network structure.

From the above review, it can see that the underdetermination issue and the identification bias issue are addressed separately in existing literature. In this work, we propose a systematic scheme that can reduce the bias in damage identification through a measurement selection method. It is found that particular combinations of available natural frequencies can significantly reduce the estimation bias compared with using all available ones. The proposed method contains three algorithms. In the first algorithm, L_1 - norm regularization is adopted with iterative random matrix multiplication and majority voting. The idea of matrix randomization is to multiply random Gaussian matrix to the linear system to achieve 1) matching of correlation structures of error terms and 2) unique solution of L_1 minimization. The majority voting process helps to estimate the damage severities from multiple iterations. In the second algorithm, the estimated damage locations are updated by removing locations with negligible damage severities. The estimated errors of natural frequencies are derived based on the estimated damage parameters, and are further adopted for natural frequency selection by a least squares method in the third algorithm. There are several advantages of the proposed the algorithm. First, the regular L_1 - norm regularization is modified to enhance the quality of damage estimation for measurement selection. Second, since the algorithm requires no additional physical modification (e.g., added mass or integrated piezoelectric circuits) of the structures, it can be used in many practical scenarios. It is worth mentioning that the proposed algorithm can also be extended for natural frequencies selection in the physical modified structures for better damage estimation. Third, the proposed algorithm is

easy to implement without deriving high order terms in the approximation. Thus, it is computationally friendly for practical uses.

The rest of the paper is organized as follows. Section 2 introduces the linear approximation of the inverse analysis of eigenvalue problem. Section 3 introduces the L_1 - norm regularization with iterative random matrix multiplication and majority voting. Section 4 introduces the proposed algorithm for bias reduction through measurement selection. Section 5 presents the case studies to validate the proposed method. Section 6 further discusses the factors that influence the performance of the algorithm. Section 7 concludes the paper.

2. Problem Formulation

For the sake of clarity, the linear approximation of the inverse analysis of eigenvalue problem is first introduced for damage identification purpose. Without loss of generality, in this research, it is considered the structural damage that induces the change of structural stiffness [17]. Also, it is assumed that only a very small number of damages occur in the structure simultaneously which is the usual case in practice.

The dynamics of an un-damped structural system can be described by the linear equation

$$\mathbf{M}\ddot{\mathbf{x}}(t) + \mathbf{K}\mathbf{x}(t) = \mathbf{F}(t) \tag{1}$$

where \mathbf{M} and \mathbf{K} are the global mass and stiffness matrices, respectively, \mathbf{x} and \mathbf{F} contain the nodal displacements and nodal forces, respectively. The eigenvalue problems associated with the healthy structure and damaged structure are shown in Eq. (2) and (3), respectively:

$$(\mathbf{K} - \lambda_i \mathbf{M}) \mathbf{\phi}_i = 0 \tag{2}$$

$$\left(\mathbf{K}^d - \lambda_i^d \mathbf{M}\right) \mathbf{\Phi}_i^d = 0, \tag{3}$$

where λ_i and $\mathbf{\phi}_i$ are the *i*th eigenvalue (squared of the *i*th natural frequency) and eigenvector of the healthy structure, and λ_i^d and $\mathbf{\phi}_i^d$ are the *i*th eigenvalue and eigenvector of the damaged structure, respectively. The damages are only induced by the loss of stiffness, so the mass matrix \mathbf{M} remains unchanged. The stiffness matrix \mathbf{K}^d of the damaged structure can be expressed as the increment $\Delta \mathbf{K}$ from \mathbf{K} in the healthy structure:

$$\mathbf{K}^d = \mathbf{K} + \Delta \mathbf{K} \tag{4}$$

Similarly, the change in eigenvalues and eigenvectors can be expressed as:

$$\lambda_i^d = \lambda_i + \Delta \lambda_i \tag{5}$$

$$\mathbf{\Phi}_i^d = \mathbf{\Phi}_i + \Delta \mathbf{\Phi}_i \tag{6}$$

Substituting Eq. (4)-(6) in to Eq. (3) and neglecting the high order terms, the first order (linear) approximation of the mapping from stiffness to natural frequencies is:

$$\Delta \lambda_i \approx \frac{\mathbf{\phi}_i^T \Delta \mathbf{K} \mathbf{\phi}_i}{\mathbf{\phi}_i^T \mathbf{M} \mathbf{\phi}_i} \tag{7}$$

In most cases, the eigenvectors are mass normalized, thus, $\mathbf{\Phi}_i^T \mathbf{M} \mathbf{\Phi}_i = 1$.

The increment $\Delta \mathbf{K}$ is expressed as the summation of elemental stiffness matrix change:

$$\Delta \mathbf{K} = \sum_{j=1}^{n} \Delta \alpha_j \, \mathbf{K}_i^{(e)}, \tag{8}$$

where $\mathbf{K}_{j}^{(e)}$ is the *j*th elemental stiffness matrix, and $\Delta \alpha_{j}$ is the damage parameter ranging in [-1,0] indicating the percentage change of stiffness of the *j*th element, where zero means no stiffness loss and -1 means the complete stiffness loss at the element, respectively. n is the number of elements in the finite element model.

Combining Eq. (7) and (8), the matrix formulation of the linear expression of the change of eigenvalues due to damage occurrence can be expressed as:

$$\Delta \lambda = \mathbf{S} \Delta \alpha + \mathbf{e}(\Delta \alpha) \tag{9}$$

where $\Delta \lambda = [\Delta \lambda_1, \Delta \lambda_2, ... \Delta \lambda_m]^T$ is the set of eigenvalue difference between the damaged structure and the healthy structure. The number m indicates the number of available natural frequencies in the measurement. $\Delta \alpha = [\Delta \alpha_1, \Delta \alpha_2, ... \Delta \alpha_n]^T$ is the set of n damage parameters. **S** is the sensitivity matrix representing the sensitivity of eigenvalues to the changes in stiffness loss. $\mathbf{e}(\Delta \alpha)$ is the error in the linearization. The components in **S** are:

$$\mathbf{S}(i,j) = \frac{\mathbf{\Phi}_i^T \mathbf{K}_j^{(e)} \mathbf{\Phi}_i}{\mathbf{\Phi}_i^T \mathbf{M} \mathbf{\Phi}_i}$$

In general, the number of columns, n, is much larger than the number of rows, m, i.e., $n \gg m$.

In practice, Eq. (9) is approximated by Eq. (10).

$$\Delta \lambda \approx S \Delta \alpha$$
 (10)

However, as mentioned in the introduction section, there are two major challenges in damage identification based on Eq. (10). First, **S** is a wide rectangular matrix so that Eq. (10) is an underdetermined system. Second, Eq. (10) is just a linear approximation of the true underlying relationship. As a result, there will be bias in the solution obtained using Eq. (10). We propose two techniques to addresses these challenges, which are described in Section 3 and 4, respectively.

3. L₁ Penalty with Iterative Random Matrix Multiplication and Majority Voting Process

We follow the common idea in the literature to address the underdetermined system, i.e., apply a penalty of L_1 norm of $\Delta \alpha$ to the solution. Instead of directly solving Eq. (9), the following optimization problem is considered:

$$\min \|\Delta \lambda - \mathbf{S} \Delta \alpha\|_{2} + \beta \|\Delta \alpha\|_{1}, \text{ s. t.} -1 \le \Delta \alpha \le 0$$
(11)

where β is the regularization parameter controlling the weight of the penalty. In practice, Eq. (11) is often solved by the following equivalent expression [18]:

$$\min \|\Delta \boldsymbol{\alpha}\|_{1}, \text{ s. t. } \|\Delta \boldsymbol{\lambda} - \mathbf{S} \Delta \boldsymbol{\alpha}\|_{2} \le \epsilon, -1 \le \Delta \boldsymbol{\alpha} \le 0$$
 (12)

where ϵ indicates the error tolerance and plays the equivalent role of β .

There are many algorithms to solve the optimization problem in Eq. (12) efficiently. However, solutions to Eq. (12) may not be sparse enough [19] to recover the true non-zero damage locations. In other words, even if adding L_1 penalty results in sparse solution, the solution may be still "abundant" compared to the underlying truth. In practice, an iterative reweighed L_1 minimization algorithm [19] is often adopted to enhance the sparsity. For reader's convenience, we quote the algorithm from [19] in Table A-1 in the appendix. There are several remarks of the algorithm: (i) Instead of minimizing Eq. (12), the algorithm can recover the underlying sparsity correctly. And (ii) The weights are updated iteratively in step 3. The update equation can adopt different forms as

discussed in [19]. The general idea of this algorithm is to increase the weights for variables estimated with small absolute values in order to push these variables to be 0 in future iterations. In this paper, the similar scheme of this idea is adopted but with different approaches as described in Algorithms 1 and 2 below.

Instead of solving Eq. (12), the following problem is solved iteratively in the proposed algorithm:

$$\min \|\Delta \boldsymbol{\alpha}\|_{1}, \text{ s. t. } \|\widetilde{\Delta \boldsymbol{\lambda}} - \widetilde{\mathbf{S}} \Delta \boldsymbol{\alpha}\|_{2} \le \epsilon, -1 \le \Delta \boldsymbol{\alpha} \le 0$$
 (13)

where $\widetilde{\Delta \lambda} = \Phi \Delta \lambda$ and $\widetilde{S} = \Phi S$ and Φ is an $m \times m$ random matrix, whose components are independent and identically distributed samples from a Gaussian distribution. The key benefit to solve Eq. (13) compared to solve Eq. (12) is that: the correlated structure of the error terms in the linear relationship is addressed.

It is known that the optimization problems in Eq. (12) and Eq. (11) are equivalent. If the penalty term in Eq. (11) is ignored, then the objective function of Eq. (11) is identical to the objective function for a regular least squares problem. In other words, if the penalty term in Eq. (11) is ignored, then the solution to (11) will be the regular least squares solution. One important assumption on regular least squares method is that the error term in the model is homogeneous, i.e., the covariance of the term **e** is a diagonal matrix and the diagonal elements are the same. This is certainly an unrealistic assumption because the term $\mathbf{e}(\Delta \alpha)$ includes both measurement error and the systematical error in the linear approximation. It is known that regular least squares method will lead to systematic bias in the solution for a system with heterogeneous errors [20]. In the proposed algorithm, the objective function Eq. (13) ignoring the penalty term is equivalent to $\left(\widetilde{\Delta\lambda} - \widetilde{S}\Delta\alpha\right)^T \left(\widetilde{\Delta\lambda} - \widetilde{S}\Delta\alpha\right) = (\Delta\lambda - S\Delta\alpha)^T (\Phi^T\Phi)(\Delta\lambda - S\Delta\alpha) \ , \ \text{ which is in the form of the}$ objective function of a generalized least square (GLS) problem [21] assuming the covariance matrix of **e** is $(\Phi^T\Phi)^{-1}$. GLS is an effective way to adjust the solution of linear systems to reduce the bias when the heterogeneous errors occur. In practice, $(\Phi^T\Phi)^{-1}$ will not be exactly the true covariance of e and further, the solution of Eq. (13) is not obtained through GLS method, but rather through the optimization with the penalty term. However, the above intuitive understanding can provide some justification on the proposed algorithm, i.e., iteratively solving Eq. (13) with different random matrices Φ s followed by the majority voting process. The underlying intuition is that when $(\Phi^T\Phi)^{-1}$ is close to the true covariance structure of the error term, then the solution of Eq. (13) will be consistent and close to the true underlying value. On the other hand, when $(\Phi^T\Phi)^{-1}$ is far from the true covariance structure of the error term, the solution will be scattered around. As a result, if different Φ s are repeatedly tried, then the solutions that are close to the true underlying value will stand out in the followed majority voting process. Indeed, similar idea has been reported in the literature when solving a sparse system [1].

Note that, the reweighed L_1 minimization algorithm in Table A-1 still applies the standard L_2 norm, and thus the solution to the reweighed L_1 minimization may be less reliable due to the heterogeneous errors. The ideas of iterative random matrix multiplication and the majority voting procedure are summarized in Algorithm 1 in Table 1. The iterative random matrix multiplication step returns an estimated matrix $\left[\widetilde{\Delta\alpha}\right]_{n\times L}$, whose column (i.e., $\widetilde{\Delta\alpha}_{l,l}$) is the estimated damage under each random matrix Φ_l . The row of $\left[\widetilde{\Delta\alpha}\right]_{n\times L}$ (i.e., $\widetilde{\Delta\alpha}_{l,l}$) records the estimations for each element through L iterations. Based on our experiences, a L of several hundreds is sufficient to achieve good results while balancing the computational time.

In the majority voting step, $P(\widetilde{\Delta\alpha_{i,\cdot}} \geq -0.05)$ is the probability that the estimated damage of the *i*th element is no less than -0.05 (i.e., a light damage). The "if" condition states that if 95% of the estimated damage severity $\widetilde{\Delta\alpha_{i,l}}$ is larger than -0.05 among L iterations, the *i*th element is treated as a healthy element and is then set to be 0 (i.e., $\widehat{\Delta\alpha_i} = 0$). In practice, only the stiffness loss larger than 5% (i.e., $\Delta\alpha_i < -0.05$) is treated as damage [3]. The threshold 95% is the confidence to reject the hypothesis that the element has stiffness loss larger than 5% at level 0.05, which is a commonly used criterion in practices [22]. Damaged elements have the majority of $\widetilde{\Delta\alpha_{i,\cdot}}$ significantly differ from 0 and the distribution of $\widetilde{\Delta\alpha_{i,\cdot}}$ often forms a unimodal shape. The mean value of all iterations are used as the estimation of damage severity.

Table 1. Algorithm 1: Iterative Random Matrix Multiplication and Majority Voting

```
Iterative Random Matrix Multiplication

For l = 1, 2, ..., L
Generate random matrix \mathbf{\Phi}_l and compute \widetilde{\Delta \lambda} = \mathbf{\Phi}_l \Delta \lambda and \widetilde{\mathbf{S}} = \mathbf{\Phi}_l \mathbf{S}
Solve Eq. (13) and record the estimation \widetilde{\Delta \alpha}_{.,l} = \left[\widetilde{\Delta \alpha}_{1,l}, \widetilde{\Delta \alpha}_{2,l}, ... \widetilde{\Delta \alpha}_{n,l}\right]^T
End

Majority Voting

Define \widetilde{\Delta \alpha}_{i.} = \left[\widetilde{\Delta \alpha}_{i,1}, \widetilde{\Delta \alpha}_{i,2}, ... \widetilde{\Delta \alpha}_{i,L}\right] and \widehat{\Delta \alpha} = \left[\widetilde{\Delta \alpha}_{1,} \widetilde{\Delta \alpha}_{2}, ..., \widetilde{\Delta \alpha}_{n}\right]
For i = 1, 2, ..., n

if P(\widetilde{\Delta \alpha}_{i.} \geq -0.05) \geq 95\%
\widehat{\Delta \alpha}_i = 0
else
\widehat{\Delta \alpha}_i = \text{mean}(\widetilde{\Delta \alpha}_{i.})
end
End
Return \widehat{\Delta \alpha} and the locations \mathbf{L}(\widehat{\Delta \alpha}) for \widehat{\Delta \alpha}_i = 0
```

Besides the estimation $\widehat{\Delta \alpha}$, Algorithm 1 also returns the locations of zero elements in $\widehat{\Delta \alpha}$, represented by $\mathbf{L}(\widehat{\Delta \alpha})$. In order to recover the damage locations accurately, an iterative procedure is proposed as Algorithm 2 in Table 2.

Table 2. Algorithm 2: Damage Location Identification Algorithm

```
    Set the iteration count q = 0, L<sup>(q)</sup> = L(Δα<sup>(q)</sup>) and L<sup>(0)</sup> = φ
    Run Algorithm 1 with constrains Δα<sub>L<sup>(q)</sup></sub> = 0 in Eq. (13), return Δα<sup>(q+1)</sup>
    Update the sparsity
        L<sup>(q+1)</sup> = L(Δα<sup>(q+1)</sup>)
    Terminate if L<sup>(q+1)</sup> = L<sup>(q)</sup> or q attains the maximum number. Otherwise, increment q and go to step 2.
    Return Δα and L(Δα) from the last iteration
```

In most cases, it takes q=2 or 3 to terminate the algorithm. The $\widehat{\Delta\alpha}$ of the last iteration is used as the final estimation of the damage parameters with the sparsity shown in $\mathbf{L}(\widehat{\Delta\alpha})$. The estimation $\widehat{\Delta\alpha}$ is named as L_1 -IMR (iteratively matrix randomization). In general, the L_1 -IMR estimation achieves better solution quality compared with the pure L_1 regularization by Eq. (12). The L_1 -IMR estimation for natural frequency selection is used in the next section.

It is interesting to compare Algorithm 2 with the reweighed L_1 minimization algorithm in Table A-1 in the appendix to see the analogy. In fact, adding constrains $\Delta \alpha_{\mathbf{L}^{(q)}} = \mathbf{0}$ in Eq. (13) is equivalent to modify the weight as:

$$w_i^{(q+1)} = \begin{cases} 1, & \widehat{\Delta\alpha}_i^{(q)} \neq 0 \\ \infty, & \widehat{\Delta\alpha}_i^{(q)} = 0 \end{cases}$$

in the reweighed L_1 minimization algorithm. In this updating step, all zero valued elements will retain as 0 in the following iterations, while all non-zero valued elements will be estimated with equal weight of 1. The condition $w_i^{(q+1)} = \infty$, for $\widehat{\Delta \alpha}_i^{(q)} = 0$ is equivalent to set $\delta = 0$ in the original weight update equation in Table A-1. The key difference between Algorithm 2 and the reweighed L_1 minimization algorithm is in step 2. Instead of solving the L_1 minimization problem once, Algorithm 1 solve the problem multiple times with different random matrices. The benefits of such approach are discussed above.

4. Measurement Selection for Bias Reduction

Even if Algorithms 1 and 2 enhance the solution quality for damage identification, the bias introduced by the linear approximation in Eq. (9) is not addressed. It is found that some subsets of available natural frequencies can return less biased estimation compared with that using all available natural frequencies. Thus, a natural frequencies selection is desired to reduce the bias in the damage estimation.

Mathematically, a subgroup of natural frequencies needs to be found to minimize the following L_2 - norm

$$d^{(k)} = \left\| \widehat{\Delta \alpha}^{(k)} - \Delta \alpha^{\text{truth}} \right\|_{2} \tag{14}$$

where $\Delta \alpha^{\text{truth}}$ is the underlying truth of the damage and $\widehat{\Delta \alpha}^{(k)}$ is the damage estimation based on the k th combination of selected natural frequencies by solving $\min \|\Delta \alpha\|_1$, s. t. $\|\Delta \lambda^{(k)} - \mathbf{S}^{(k)} \Delta \alpha\|_2 \le \epsilon$, $-1 \le \Delta \alpha \le 0$. $\lambda^{(k)}$ and $\mathbf{S}^{(k)}$ are the eigenvalue difference and sensitivity matrix corresponding to the kth combination of selected natural frequencies, respectively. In other words, $\Delta \lambda^{(k)}$ and $\mathbf{S}^{(k)}$ are the sub-vector and sub-matrix of $\Delta \lambda$ and \mathbf{S} by retaining the rows corresponding to the kth combination of selected natural frequencies. For example, if \mathbf{S} has dimension 7×20

(i.e., 7 natural frequencies and 20 elements), the submatrix $\mathbf{S}^{(k)}$ will have less rows but the same number of columns, i.e., if only 4 natural frequencies are selected as system measurements, the dimension of $\mathbf{S}^{(k)}$ will be 4×20 . Please note for m available natural frequencies, there are total $2^m - 1$ different combinations.

The challenges in this problem are from the following aspects. First, the underlying truth $\Delta \alpha^{\text{truth}}$ is unknown. Thus, Eq. (14) cannot be used directly for bias comparison. Second, since the sensitivity matrix **S** is obtained from the linear approximation, the following optimization problems are not equivalent,

$$\arg_k \min \|\Delta \lambda^{(k)} - \mathbf{S}^{(k)} \Delta \alpha\|_2 \iff \arg_k \min \|\widehat{\Delta \alpha}^{(k)} - \Delta \alpha^{\text{truth}}\|_2$$

A reasonable approach is to derive an approximation of the incomputable quantity $d^{(k)}$ in Eq. (14). $b^{(k)}$ is proposed to be an approximation of $d^{(k)}$, where $b^{(k)}$ is defined as $\left\|\left(\underline{\mathbf{S}^{(k)}}^{\mathbf{T}}\underline{\mathbf{S}^{(k)}}\right)^{-1}\underline{\mathbf{S}^{(k)}}^{\mathbf{T}}\mathbf{e}^{(k)}\right\|_{2}$. The details and the rational of this approximation are discussed below.

First note, the eigenvalue difference $\Delta\lambda$ can be expressed with the underlying damages $\Delta\alpha^{\rm truth}$ and the error term **e**:

$$\Delta \lambda = \mathbf{S} \Delta \alpha^{\text{truth}} + \mathbf{e} \tag{15}$$

Similarly, the eigenvalue difference for the kth combination of selected natural frequencies is:

$$\Delta \lambda^{(k)} = \mathbf{S}^{(k)} \Delta \alpha^{\text{truth}} + \mathbf{e}^{(k)}$$
 (16)

where $\mathbf{e}^{(k)}$ measures the error in the eigenvalue difference corresponding to the kth combination. Please note Eq. (15) and (16) are exact without approximations.

Intuitively, if $\mathbf{e}^{(k)} \to \mathbf{0}$, solving $\Delta \lambda^{(k)} = \mathbf{S}^{(k)} \Delta \alpha$ returns the unbiased estimation of $\Delta \alpha^{\text{truth}}$. Thus, it is reasonable to select the natural frequencies with small magnitudes in \mathbf{e} to form the combination. However, such an approach does not take the structure of the sensitivity matrix into consideration. An ill-conditioned sensitivity matrix may result in large estimation errors. The sensitivity matrix \mathbf{S} can be simplified by removing the columns that corresponding to the healthy

elements that are identified by Algorithm 2. $\underline{\mathbf{S}}$ is denoted as the simplified sensitivity matrix by removing columns corresponding to the zero elements in $\widehat{\Delta \alpha}$, represented by $\mathbf{L}(\widehat{\Delta \alpha})$. For example, if \mathbf{S} has dimension 7×20 and only two unhealthy elements are identified, then the submatrix $\underline{\mathbf{S}}$ will be 7×2 by removing all columns that correspond to the healthy elements. Eq. (16) can be rewritten as:

$$\Delta \lambda^{(k)} = \mathbf{S}^{(k)} \Delta \alpha^{\text{truth}} + \mathbf{e}^{(k)}$$
(17)

where $\Delta\underline{\alpha}^{\text{truth}}$ is the subset of $\Delta\alpha^{\text{truth}}$ with non-zero valued components and $\underline{\mathbf{S}}^{(k)}$ is the submatrix of $\mathbf{S}^{(k)}$ by removing the columns corresponding to zero elements in $\Delta\alpha^{\text{truth}}$. Following the previous examples, if $\mathbf{S}^{(k)}$ has dimension 4×20 , then $\underline{\mathbf{S}}^{(k)}$ is 4×2 . It is worth to point out that the number of selected natural frequencies should be larger than the number of nonzero elements in $\Delta\underline{\alpha}^{\text{truth}}$ so that $\underline{\mathbf{S}}^{(k)}$ will be a square or tall matrix. Eq. (17) can be re-written as

$$\underline{\mathbf{S}}^{(k)} \Delta \underline{\alpha}^{\text{truth}} = \Delta \lambda^{(k)} - \mathbf{e}^{(k)}$$
(18)

According to Eq. (18), it can be seen that $\mathbf{e}^{(k)}$ does not impacts on $\Delta \underline{\alpha}^{\text{truth}}$ directly, rather, through the matrix of $\underline{\mathbf{S}}^{(k)}$. More specifically, the solution of $\Delta \underline{\alpha}^{\text{truth}}$ based on (18) is:

$$\Delta \underline{\alpha}^{\text{truth}} = \left(\underline{\mathbf{S}^{(k)}}^{\mathsf{T}} \underline{\mathbf{S}^{(k)}}\right)^{-1} \underline{\mathbf{S}^{(k)}}^{\mathsf{T}} \Delta \lambda^{(k)} - \left(\underline{\mathbf{S}^{(k)}}^{\mathsf{T}} \underline{\mathbf{S}^{(k)}}\right)^{-1} \underline{\mathbf{S}^{(k)}}^{\mathsf{T}} \mathbf{e}^{(k)}$$
(19)

The difference between $\Delta \underline{\alpha}^{\text{truth}}$ in Eq. (19) and its approximation without knowing $\mathbf{e}^{(k)}$ is $b^{(k)} = \left\| \left(\underline{\mathbf{S}^{(k)}}^{\mathsf{T}} \underline{\mathbf{S}^{(k)}} \right)^{-1} \underline{\mathbf{S}^{(k)}}^{\mathsf{T}} \mathbf{e}^{(k)} \right\|_{2}$. Thus, $b^{(k)}$ can be used as an approximation of $d^{(k)}$. The optimal combination of natural frequencies can be chosen as $k^* = \arg_k \min b^{(k)}$.

To compute $b^{(k)}$, the value of the error term \mathbf{e} is needed. The value of \mathbf{e} can be estimated by $\hat{\mathbf{e}} = \Delta \lambda - \mathbf{S} \widehat{\Delta \alpha}$, where $\widehat{\Delta \alpha}$ is the output from Algorithm 2. To summarize, the proposed natural frequency selection algorithm is shown as Algorithm 3 in Table 3.

Table 3. Algorithm 3: Natural Frequency Selection Algorithm for Bias Reduction

RUN Algorithm 2

CALCULATE the estimated error $\hat{\mathbf{e}} = \Delta \lambda - \mathbf{S} \widehat{\Delta \alpha}$

For $k = 1, 2, ..., 2^m - 1$

CALCULATE the estimated bias $\hat{b}^{(k)}$

End

Return $k^* = \arg_k \min \hat{b}^{(k)}$ as the final combination

There are several remarks on Algorithm 3. First, $\widehat{\Delta \alpha}$ is pre-computed in Algorithm 2, so that the computational load does not explode for exhausting all possible measurement combinations. In fact, as mentioned earlier, the number of the selected natural frequency needs to be larger than the number of non-zero elements in $\widehat{\Delta \alpha}$. Thus, the actual number of combinations is further reduced. For example, if \underline{S} has dimension 7×2 , the combination should contain at least 2 natural frequencies. Second, the proposed algorithm will not guarantee the selected combination k^* is the optimal one that minimize Eq. (14) because the criteria used $b^{(k)}$ is just an approximation of $d^{(k)}$. Detailed numerical studies and discussions will be conducted to illustrate the performance of the proposed algorithms in Section 5 and 6.

In practice, it can re-do Algorithm 1 and 2 for the selected natural frequencies from Algorithm 3 to estimate the damages, where the original matrix \mathbf{S} in Algorithm 1 becomes a matrix with only the selected rows (corresponding to the selected natural frequencies) left. The estimation after this additional procedure is named as L_1 -Final to differentiate it from L_1 -IMR from Algorithm 2.

5. Case Studies and Validation

In this section, the proposed algorithm is validated using simulation for a fixed-free beam structure with setup in Figure 1.

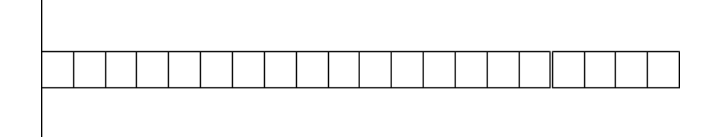


Figure 1. The fixed-free beam for the simulation. There are total 20 elements in the beam.

The system parameters are summarized in Table 4.

Table 4. Parameters of the Beam Structure

Material	Young's Modulus	Density	Length	Width	Thickness	m	n
Aluminum	$7.1 \times 10^{10} \text{ N/}m^2$	$2700 \text{kg}/m^3$	0.4184m	0.0381m	3.175mm	7	20

The beam consists 20 elements and the first 7 modes are calculated using FEM. Thus, there are total 127 different combinations of natural frequencies. In the simulation, two scenarios for a damaged beam will be considered. In the first example, the beam with two faulty elements is considered, where the stiffness loss occurs at elements 8 and 17 with $\Delta\alpha_8=-0.3$ and $\Delta\alpha_{17}=-0.1$, respectively. In the second example, a three-fault case with $\Delta\alpha_3=-0.1$, $\Delta\alpha_{10}=-0.2$ and $\Delta\alpha_{18}=-0.2$ is considered. The first seven natural frequencies are calculated for the healthy beam and the damaged beam using FEM in Table 5.

Table 5. The First Seven Natural Frequencies (Hz) (n.f.)

Order of n.f.	Healthy Beam	Two Faults	% change in n.f	Three Faults	% change in n.f
1	94.4	93.4	1.06%	93.3	1.17%
2	591.6	584.3	1.23%	583.2	1.42%
3	1657.0	1631.4	1.54%	1651.4	0.34%
4	3247.8	3225.8	0.68%	3188.6	1.82%
5	5370.5	5241.8	2.40%	5287.3	1.55%
6	8025.8	7944.3	1.02%	7821	2.55%
7	11215.3	11127.1	0.78%	11000.2	1.92%

5.1 Beam with two faulty elements

In the first example, the beam with two faulty elements is considered, where the stiffness loss occurs at elements 8 and 17 with $\Delta \alpha_8 = -0.3$ and $\Delta \alpha_{17} = -0.1$, respectively.

Figure 2 presents the bias $d^{(k)} = \left\| \widehat{\Delta \alpha}^{(k)} - \Delta \alpha^{\text{truth}} \right\|_2$ in Eq. (14) as a function of the combination index k = 1, 2, 3, ..., 127. The combination is ordered from the single natural frequency to all seven natural frequencies, i.e., $\{1, 2, 3, ..., (1, 2), (1, 3), ..., (1, 2, 3), (1, 2, 4), ..., (1, 2, 3, 4, 5, 6, 7)\}$. $\widehat{\Delta \alpha}^{(k)}$ is calculated by $\min \|\Delta \alpha\|_1$, s. t. $\|\Delta \lambda^{(k)} - \mathbf{S}^{(k)} \Delta \alpha\|_2 \le \epsilon, -1 \le \Delta \alpha \le 0$ with $\epsilon = 10^{-9}$.

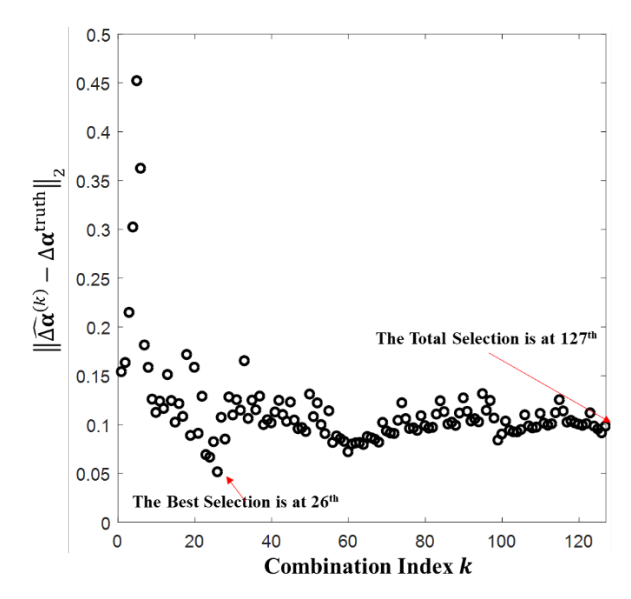


Figure 2. The bias of the estimated damages for different combinations of natural frequencies

It is clearly shown in Figure 2 that the combination of all seven natural frequencies (the 127^{th} combination) does not result in the smallest bias. In this damage scenario, the smallest bias is obtained by the 26^{th} combination of the fifth and sixth natural frequencies, i.e., (5, 6). From Figure 2, it can be seen that the bias has relatively large values for the first seven combinations. Since the first seven combinations are all single natural frequencies, the linear system is underdetermined with two faulty elements. Also, there is a jump at k = 18, (the combination of the second and the seventh natural frequencies), which is due to the correlated structure of the second and the seventh rows in **S**. As discussed in section 4, the ill-posed sensitivity matrix may result in large errors even with regularization.

Figure 3 presents the results of the histogram of the severity estimation of 20 elements from Algorithm 1.

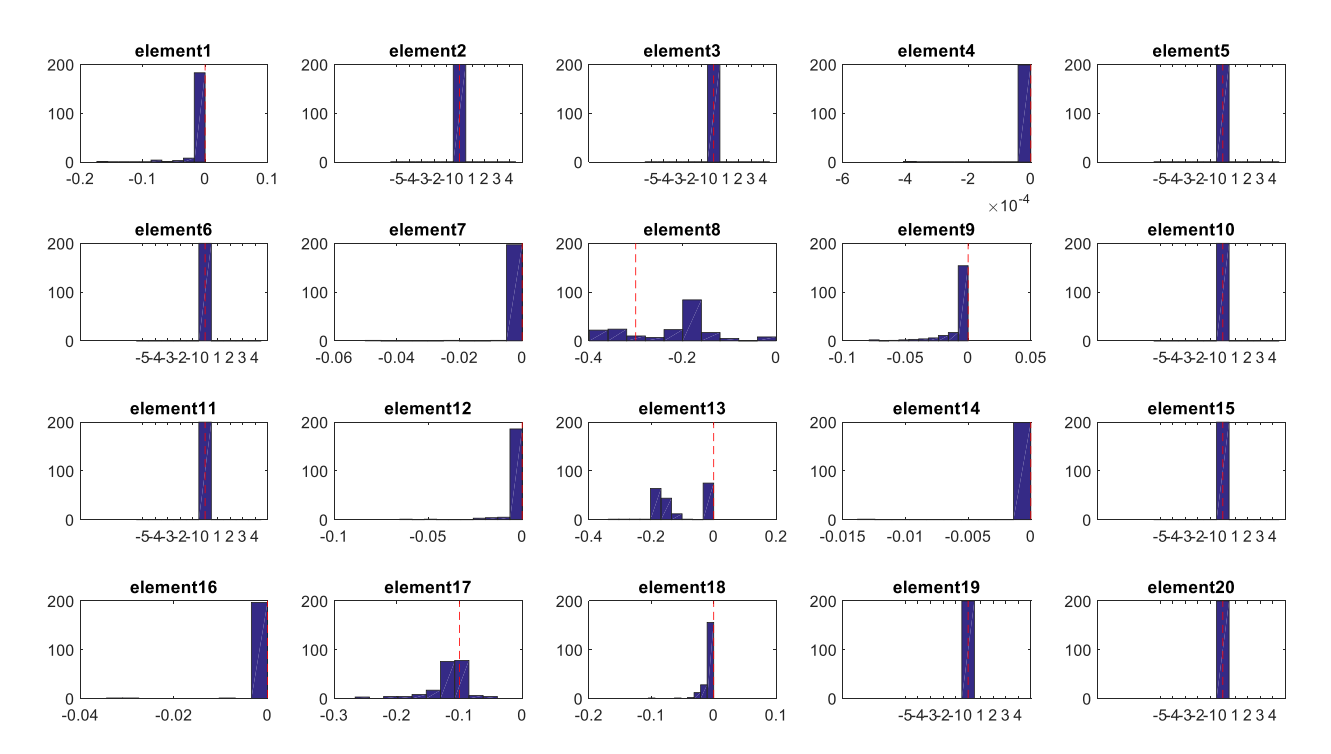


Figure 3. Damage parameter histogram of 20 elements with Algorithm 1. True damages of each element are labeled using dash lines.

In Figure 3, the true damage locations, i.e., elements 8 and 17, have histograms around the underlying true damages -0.3 and -0.1. The densities for most of other elements concentrate exactly at 0 as expected, e.g., elements 2, 6 and 10. Elements 1, 4, 9 and 18 have the majority of the density concentrate at 0 with a light tail spreading to negative values. Element 13 has density concentrate both at 0 and -0.2. It can be seen that true damage locations have densities apparently differ from 0, while non-damaged locations tend to have most density distributed at 0. These locations are set to $\Delta \hat{\alpha} = 0$ in the majority voting process.

Results obtained after Algorithm 2 are shown in Figure 4. In Figure 4, the only two non-zero distributed elements are the element 8 and 17 with density concentrated around the true damage magnitudes. The estimated damage parameters are $\widehat{\Delta \alpha}_8 = -0.33$ and $\widehat{\Delta \alpha}_{17} = -0.11$ with all other $\widehat{\Delta \alpha}_{i\neq 8 \text{ or } 17} = 0$.

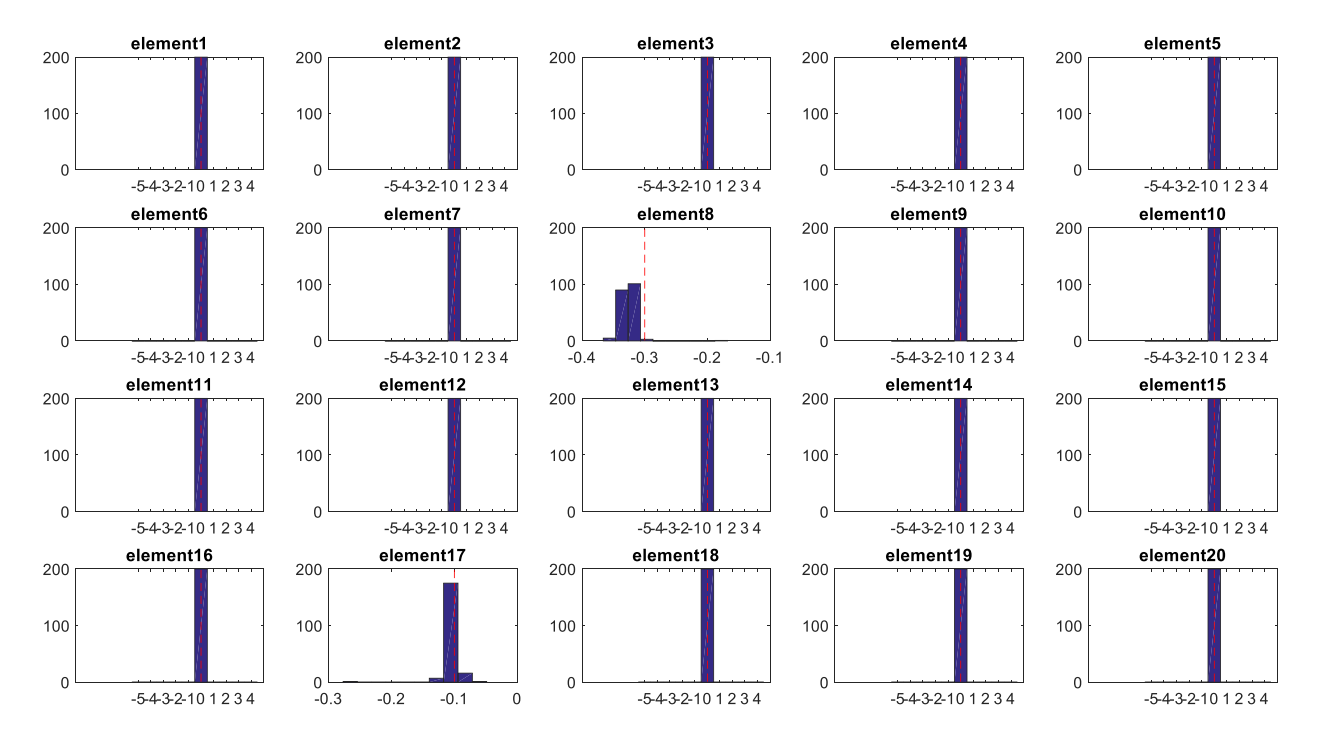


Figure 4. Damage parameter histogram of 20 elements after Algorithm 2. True damages of each element are labeled using dashed lines

The estimated bias $\hat{b}^{(k)}$ for k=8,9,...,127 are presented in Figure 5. It can be seen that $\hat{b}^{(k)}$ has very similar trend compared to $\|\widehat{\Delta\alpha}^{(k)} - \Delta\alpha^{\rm truth}\|_2$. By Algorithm 3, $k^*=26$ and the result is consistent with the smallest bias combination as shown in Figure 1. Thus, only the fifth and sixth natural frequencies are suggested to be included in the estimation of damage parameters to reduce the estimation bias. Please note that the comparison between the estimated bias $\hat{b}^{(k)}$ and the $\|\widehat{\Delta\alpha}^{(k)} - \Delta\alpha^{\rm truth}\|_2$ is only shown for $k \geq 8$. Two elements are identified as stiffness loss by Algorithm 2. In order to apply the least square method in Eq. (19), $\underline{S}^{(k)}$ should consist at least two rows, i.e., combination of at least two natural frequencies. Thus, $k \geq 8$ because the first 7 combinations only contain one natural frequency.

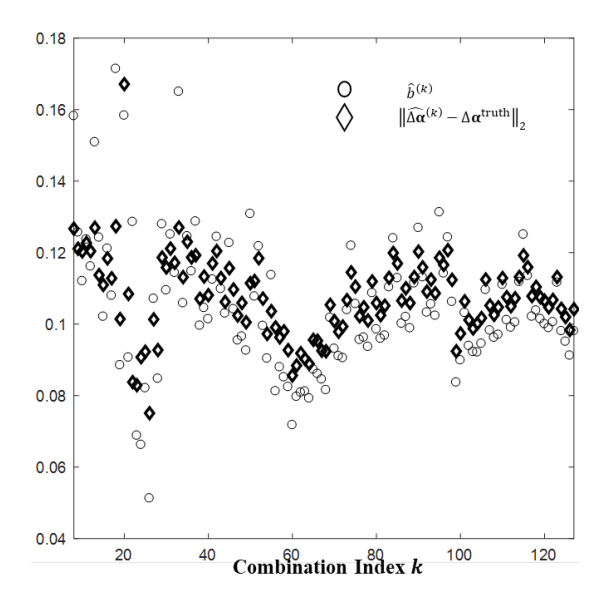


Figure 5. Plots of $\hat{b}^{(k)}$ and $d^{(k)}$ for k = 8, 9, ..., 127.

Figure 6 presents the comparison results of the damage parameter estimation using different methods.

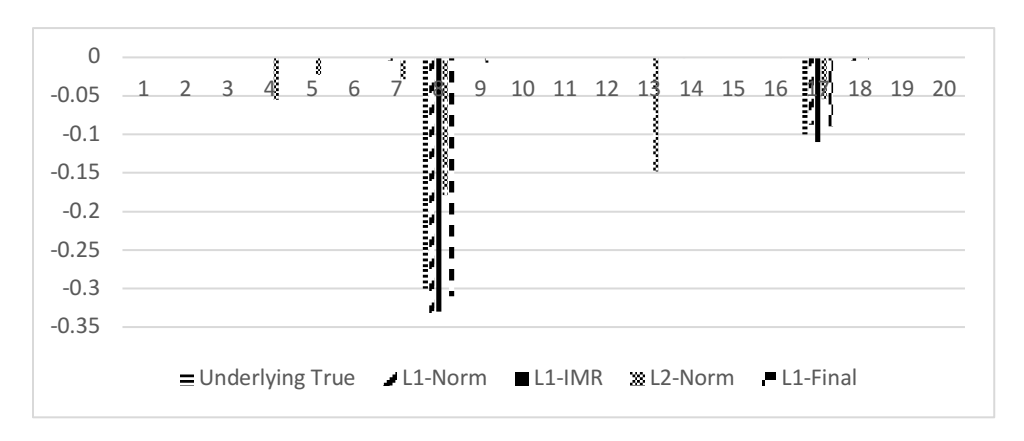


Figure 6. Comparison of damage parameter estimation using different approaches.

The L_1 - Norm method adopts Eq. (12), the L_1 -IMR adopts the proposed method with iterative matrix randomization, i.e., $\widehat{\Delta\alpha}$ by Algorithm 2 and the L_1 -Final is the estimation by re-doing Algorithms 1 and 2 using the selected natural frequencies only. The L_2 - Norm adopts Eq. (12) but with L_2 penalty. It can be seen from the comparison, the L_1 -IMR and L_1 -Final return the most accurate estimation both for the damage locations and damage severities compared to all other two methods. The L_1 -Final has a slightly better estimation compared to L_1 -IMR. The L_1 - norm method returns comparable results at the true damage locations, but also has estimation with small

magnitudes on a few healthy elements. The L_2 - norm performs the worst among all three methods with distributed estimation along elements. In practice, the L_1 -IMR is good enough for damage estimation and L_1 -Final can be further adopted if cost is allowed.

5.2 Beam with Three Faulty Elements

In the following, the proposed algorithm is adopted for a scenario with three faulty elements, where $\Delta \alpha_3 = -0.1$, $\Delta \alpha_{10} = -0.2$ and $\Delta \alpha_{18} = -0.2$. The histogram of elements after Algorithm 2 is presented in Figure 7. Similar to the case with two faulty elements, the true damage locations are identified correctly.

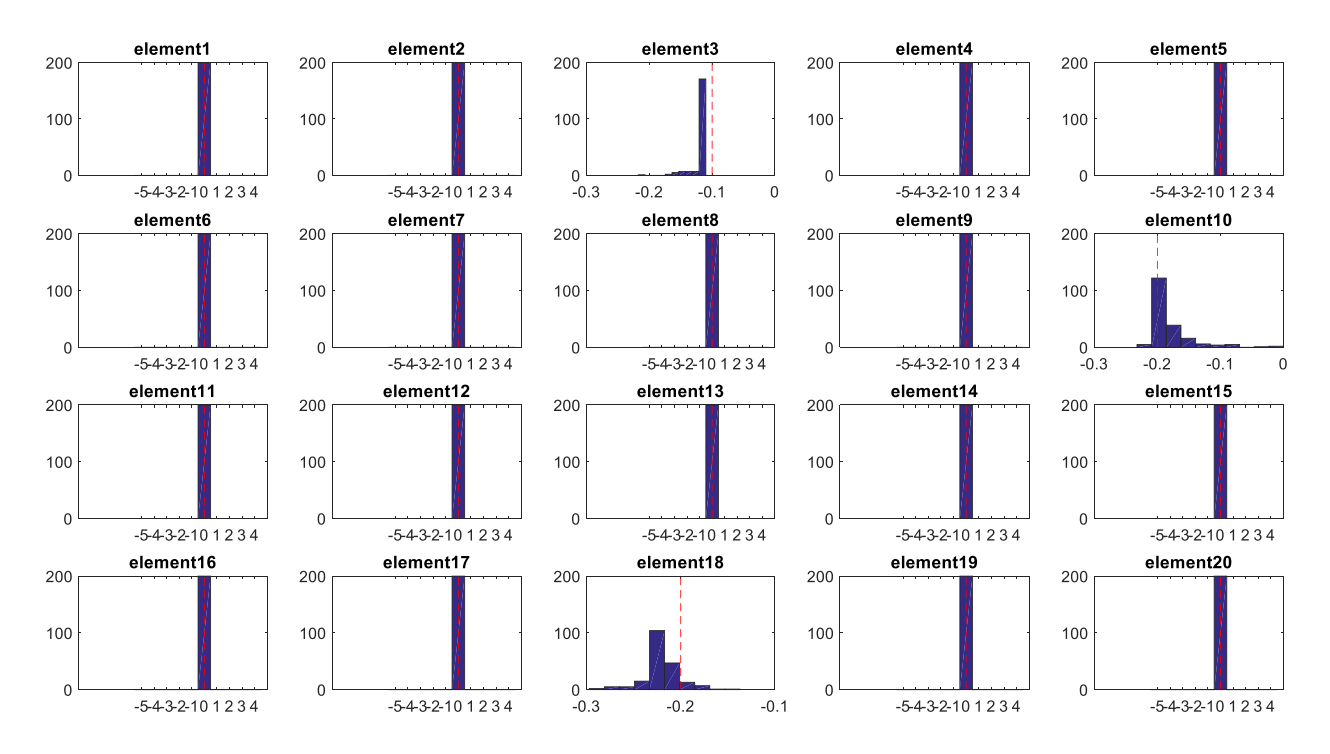


Figure 7. Damage parameter histogram of 20 elements after Algorithm 2. True damages of each element are labeled using dash lines

The comparison between $\hat{b}^{(k)}$ and the $\|\widehat{\Delta \alpha}^{(k)} - \Delta \alpha^{\text{truth}}\|_2$ is presented in Figure 8. Since three damage locations are identified, at least three natural frequencies are needed, i.e., $k \geq 29$. By Algorithm 3, $k^* = 43$ with the first, the sixth and the seventh natural frequencies is the combination with the smallest bias in the estimation. The jumpy peaks for some $\hat{b}^{(k)}$ s are due to

the correlated structure of $\underline{\mathbf{S}}^{(k)}$. In Figure 9, the comparison of damage parameter estimation is presented. The proposed L_1 -Final has the best estimation.

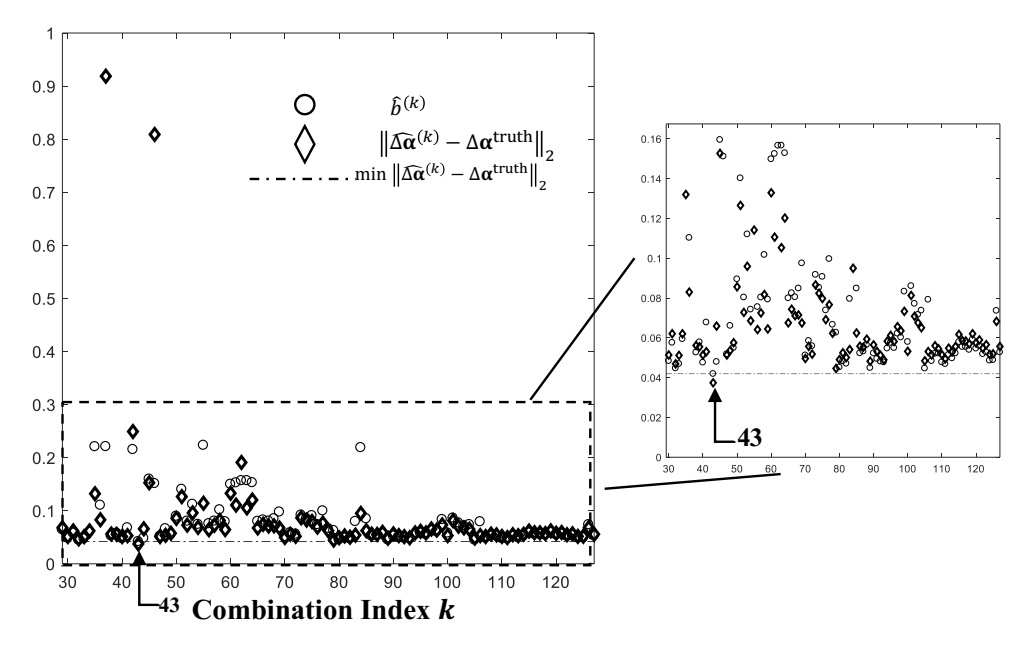


Figure 8. Plots of $\hat{b}^{(k)}$ and the $\|\widehat{\Delta \alpha}^{(k)} - \Delta \alpha^{\text{truth}}\|_2$ for $k = 29, 30, \dots, 127$.

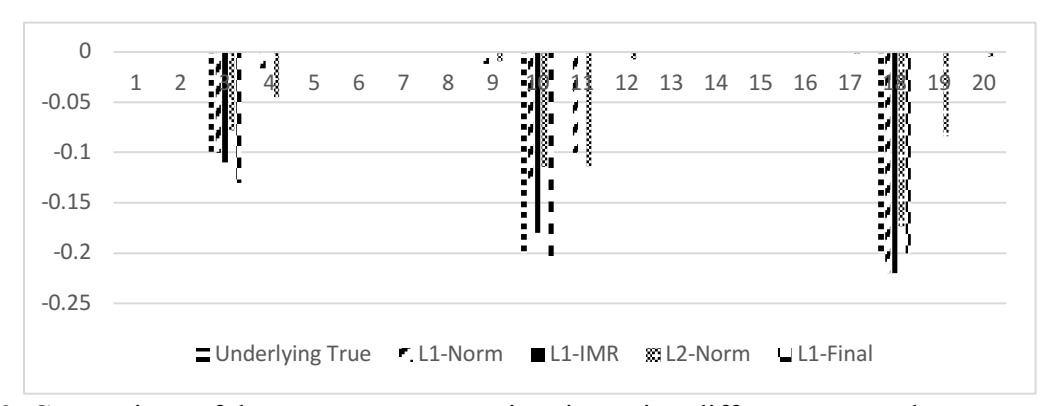


Figure 9. Comparison of damage parameter estimation using different approaches

5.3 Performance and Robustness Evaluation

In Table 6, the overall performance of the proposed algorithm in a comprehensive study is presented. The study adopts the same beam structure in previous two examples (i.e., Table 4) and exhausts all possible combinations between damage locations and damage severities for $-0.4 \le \Delta\alpha \le -0.05$ with increment 0.05. The lower bound -0.4 of $\Delta\alpha$ is an average of stiffness loss by exhausting all individual element with different level of stiffness loss to make the mean reduction

of the first seven natural frequencies about 5%. In most cases, 5% decrease in natural frequencies can be referred to a severe damage in the structure [23,24].

Table 6. Performance of the Proposed Algorithm in Different Damage Scenarios

	Single Fault	Two Faults	Three Faults
$k^* = \arg_k \min d^{(k)}$	94.3%	83.5%	80.2%
$d^{(k^*)} \le d^{(127)}$	97.1%	94.7%	91.5%
# simulations	160	12160	583680

In the simulation study, three fault scenarios have been studied, i.e., single fault, two faults and three faults. The performance is measured in two ways. 1) $k^* = \arg_k \min d^{(k)}$ indicates the selected combination k^* by Algorithm 3 is the optimal combination that minimizes the bias. It can be seen the proposed algorithm can detect the optimal combination above 80 percentage in all three damage scenarios. 2) $d^{(k^*)} \leq d^{(127)}$ indicates that the selected combination k^* has smaller bias compared with the case when all natural frequencies are used. The selected combination by the proposed algorithm can achieve smaller bias than using all seven natural frequencies over 90 percentage in all three damage scenarios. It is not surprising to see the single fault scenario has the best performance, in which case the Eq. (19) is reduced to the scalar calculation without any matrix inversion.

To test the robustness of the proposed algorithm, different levels of random noise are added to the measurements of natural frequencies. Figure 10 presents the performance of the algorithm. The accuracy is defined as true positive rate to identify the damage locations, i.e., the proportion to recover the underlying damage location by Algorithm 2. For example, the 0.81 in the single fault scenario with noise level 5% indicates 130 out 160 cases that Algorithm 2 can recover the true damage location. The 0% noise level indicates noise free case for all three scenarios. The accuracy decreases as the noise level increases. The impact of noise is greater in multiple faults case compared to the single fault case. In general, the proposed algorithm performs well for random noise level no larger than 5%, where accuracies are above 60%.

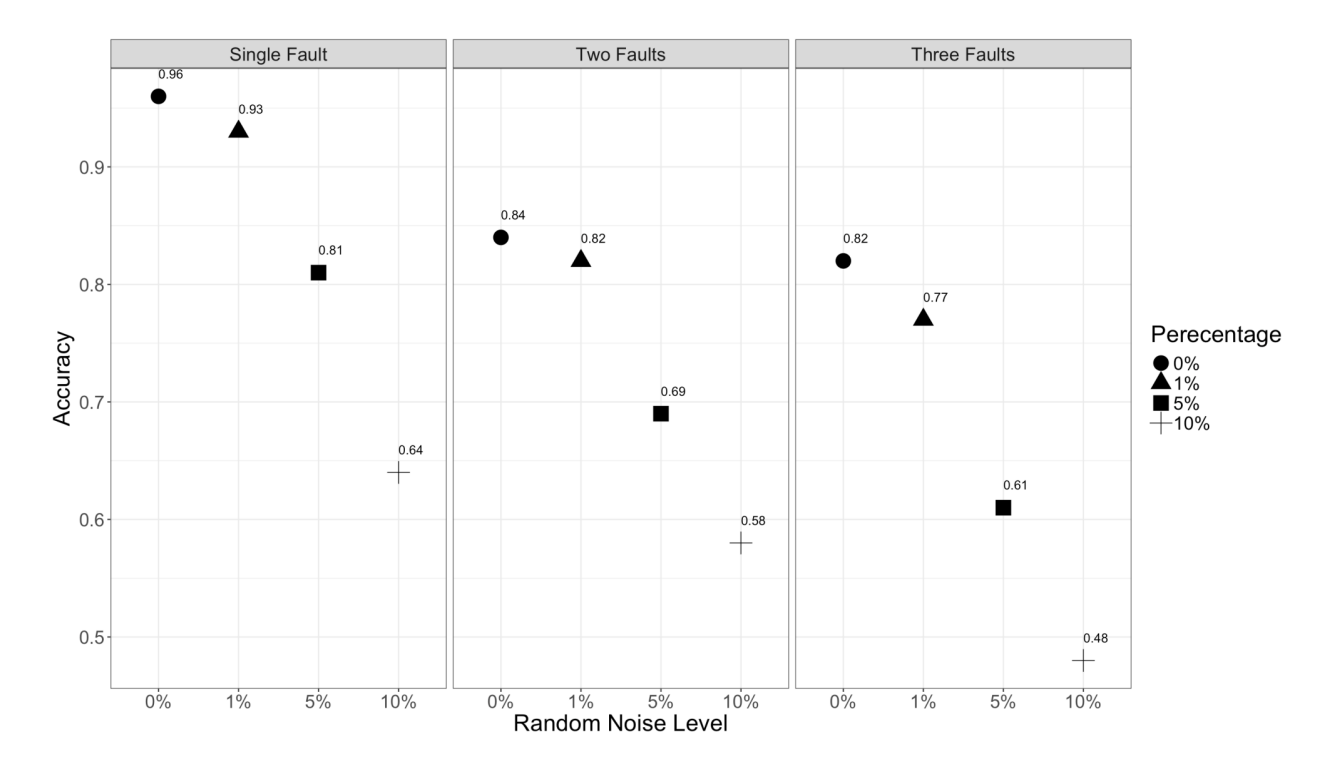


Figure 10. Accuracy of damage location identification by Algorithm 2 under random noise scenarios.

5.4 Damage Location Identification Using a FEM with 200 Elements

The accuracy of natural frequency selection by Algorithm 3 depends on the estimated damage from Algorithm 2, which is equivalent to the damage locations being identified. To further validate the performance of the proposed method for a large number of elements, we adopt the same beam structure with n=200 elements. The underlying damages are $\Delta\alpha_{40}=-0.4$ and $\Delta\alpha_{170}=-0.3$. The first seven natural frequencies are used to identify the damage locations. The results of $\Delta\alpha$ for the first, fifth and the seventh iteration (i.e., q=1,5 and 7) by Algorithm 2 are reported in Figure 11. The damage locations converge at q=7, where the true damage locations (elements 40 and 170) are recovered with the estimated values $\Delta\alpha_{40}=-0.38$ and $\Delta\alpha_{170}=-0.27$. In the first iteration, most of the estimated damages are around the true damage locations. It turns out that the true damage values are under-estimated due to this reason. A few elements (elements 1 and 50-55) have estimated values larger than -0.1. In the fifth iteration, elements that are not around the true damage locations are removed. The damage locations eventually converge at the seventh iteration.

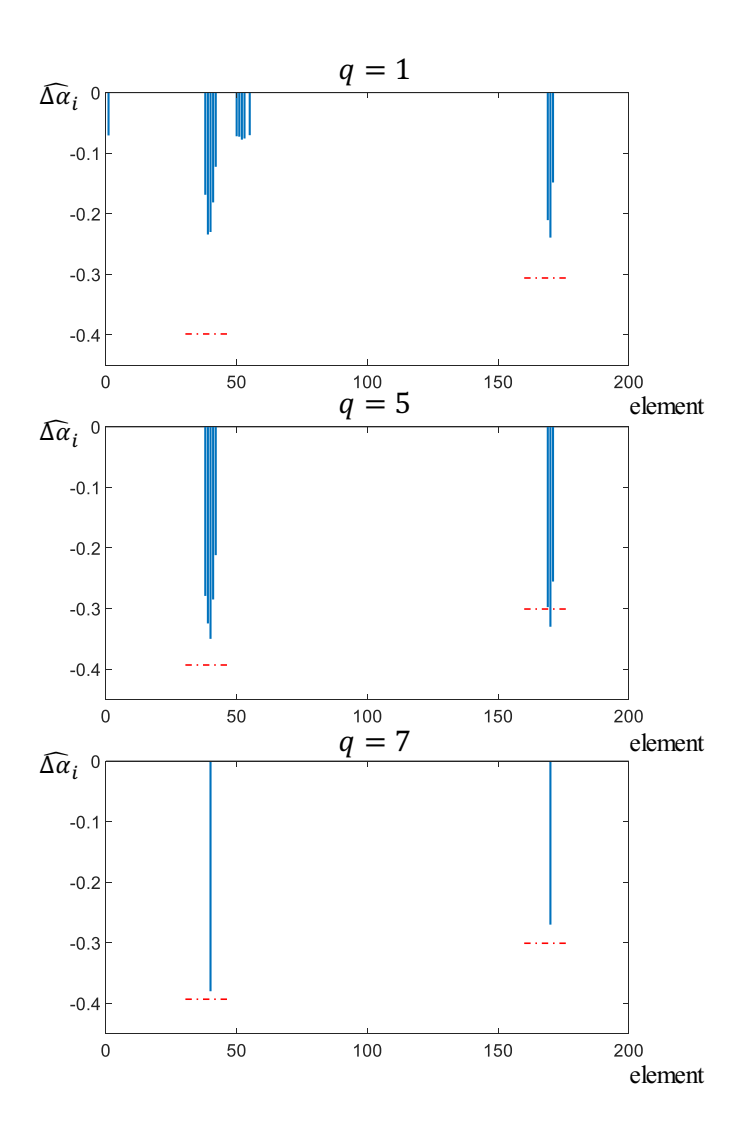


Figure 11. $\Delta \hat{\alpha}$ for each iteration q by Algorithm 2. The x-axis is 200 elements and the y-axis is $\Delta \hat{\alpha}$. The dashed lines are the underlying damage for elements 40 and 170.

5.5 Experimental Study

In this section, the proposed method is validated using a real experimental setup of a fixed-fixed beam structure [25]. The parameters of the beam are summarized in Table 7.

Table 7. Parameters of the Real Beam Structure

Material	Young's Modulus	Density	Length	Width	Thickness
Aluminum	68.9Gpa	$2700 \text{kg}/m^3$	510 mm	19.05mm	4.76mm

To mimic the stiffness loss, a small mass with weight 2.9g is added to the middle section of the beam as shown in Figure 12.

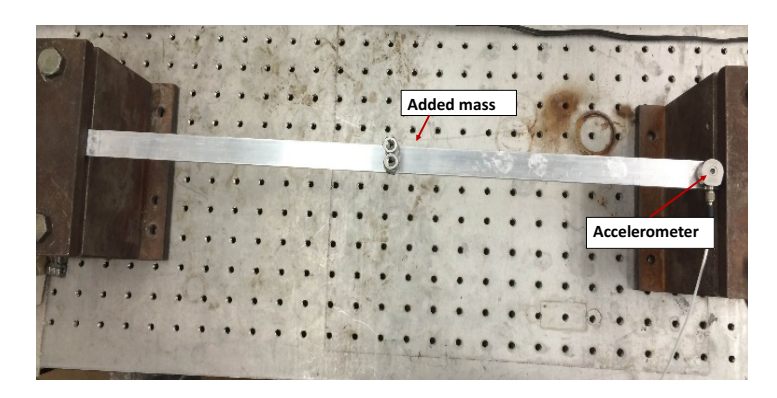


Figure 12. A small mass is attached on the middle of the beam to mimic the stiffness reduction with an accelerometer located near one end of the beam.

The first three natural frequencies of the beam are measured for both before and after mass added in Table 8.

Table 8. Natural Frequencies (Hz) Before and After Mass Added

Order of n.f.	Before Mass	After Mass	% change in n.f
1	92	89.5	2.72%
2	498	489	1.80%
3	1219	1200	1.56%

Based on the width of the small mass, the FEM of the fixed-fixed beam is designed to contain 41 elements with the 21^{st} element as faulty. The equivalent stiffness lost can be calculated as $\Delta\alpha_{21} = -0.54$ by considering model updating [8]. The proposed algorithm detects the true damage location with estimation $\widehat{\Delta\alpha_{21}} = -0.51$. The first and the third natural frequencies are selected to minimize the bias error by Algorithm 3.

6. Impact of Severe Damage and Discussion on Implementation in Practice

In this section, we first explore the influence of severe damage on the performance of the proposed algorithm. The proposed algorithm is effective on selection of natural frequencies to reduce the estimation bias. However, it does not eliminate the bias. In Figure 11, the accuracy of

linear approximation of natural frequency compared with the underlying truth is presented. The beam is set up as that in Table 4 with stiffness loss only at element 8.

Figure 13(a) presents the linear approximation of the first order natural frequency. The solid line is the underlying truth and the dashed line is the linear approximation. Since Taylor's expansion is conducted at the healthy condition, the difference between the linear approximation and the underlying truth is getting larger as $\Delta \alpha \rightarrow -1$. Figure 13(b) summarizes the accuracy of the linear approximation of the first seven modes in terms of the difference in percentage, i.e., $\Delta \lambda - \mathbf{S}^{(k)} \Delta \alpha^{\text{truth}}$

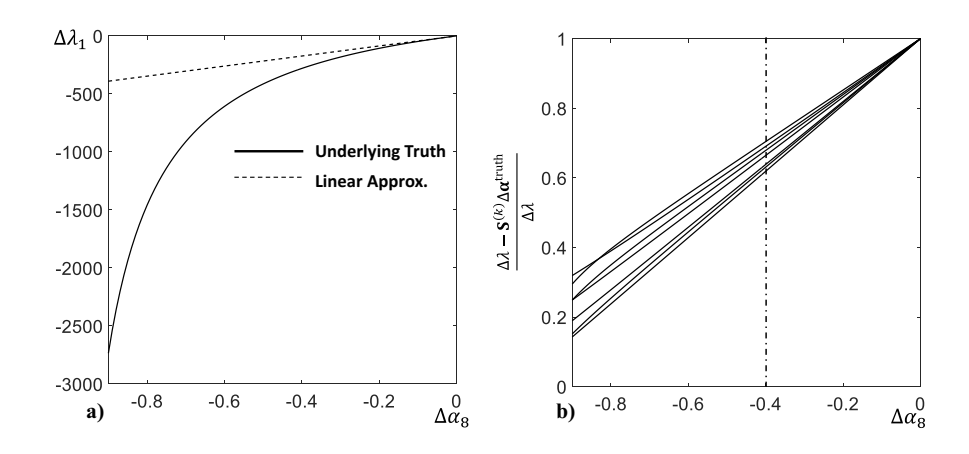


Figure 13. Accuracy of linear approximation in natural frequencies

It can be seen that the accuracy is about 60% for $\Delta\alpha=-0.4$. As the comprehensive simulation study indicated in Section 4, the proposed algorithm performs well at such accuracy level. It is worth noting that the performance of the algorithm gets worse for severe stiffness loss. Under mild damage conditions, the histogram of $\Delta\alpha$ s are close to the underlying truth but with small differences (e.g., Figure 4 and 7). For severe damage loss, such differences can be large or even the identified damage locations can be wrong. In Figure 14, an example of the histogram of $\Delta\alpha$ s after Algorithm 2 for a severe damage case $\Delta\alpha_3=-0.9$, $\Delta\alpha_{10}=-0.9$ and $\Delta\alpha_{18}=-0.2$ is presented.

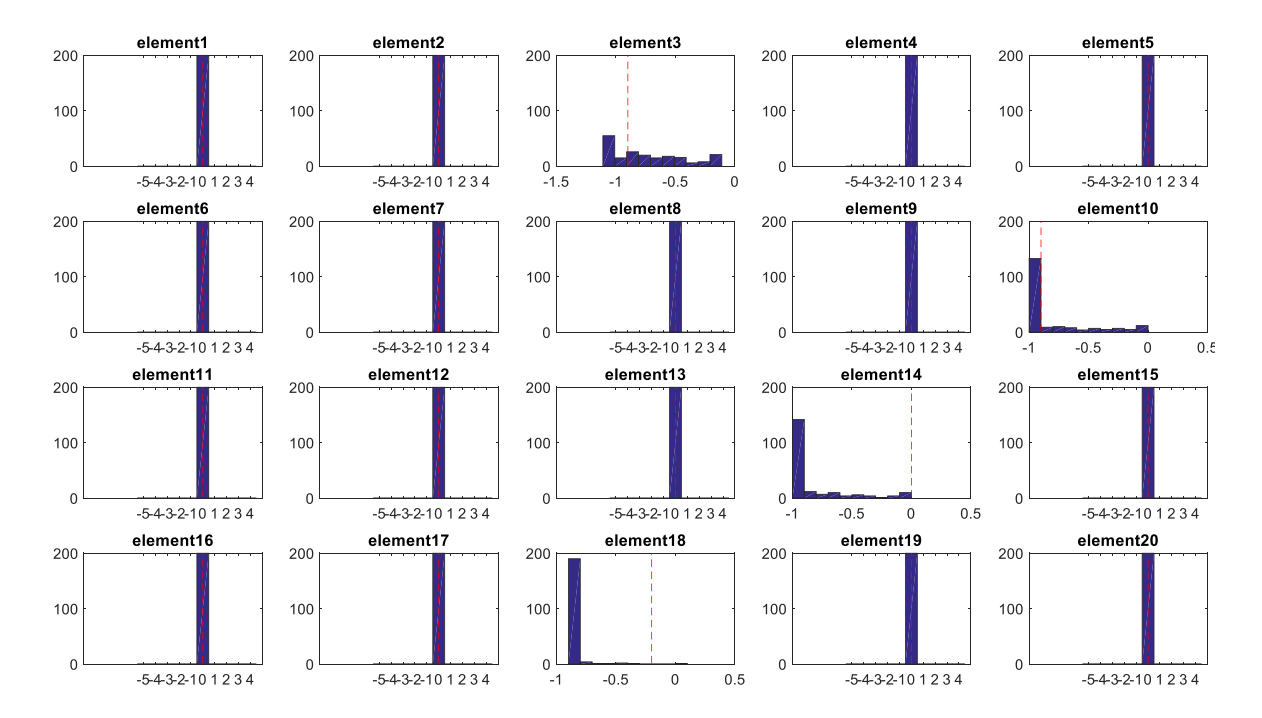


Figure 14. Damage parameter histogram of 20 elements after Algorithm 2. True damages of each element are labeled using dashed lines

All three true damage locations are identified but with an additional element 14 wrongly identified. The magnitude of stiffness loss at element 18 is estimated much smaller than the truth due to the additional element. Thus, the results of the proposed algorithm will not be informative on the selection of natural frequencies as shown in Figure 15.

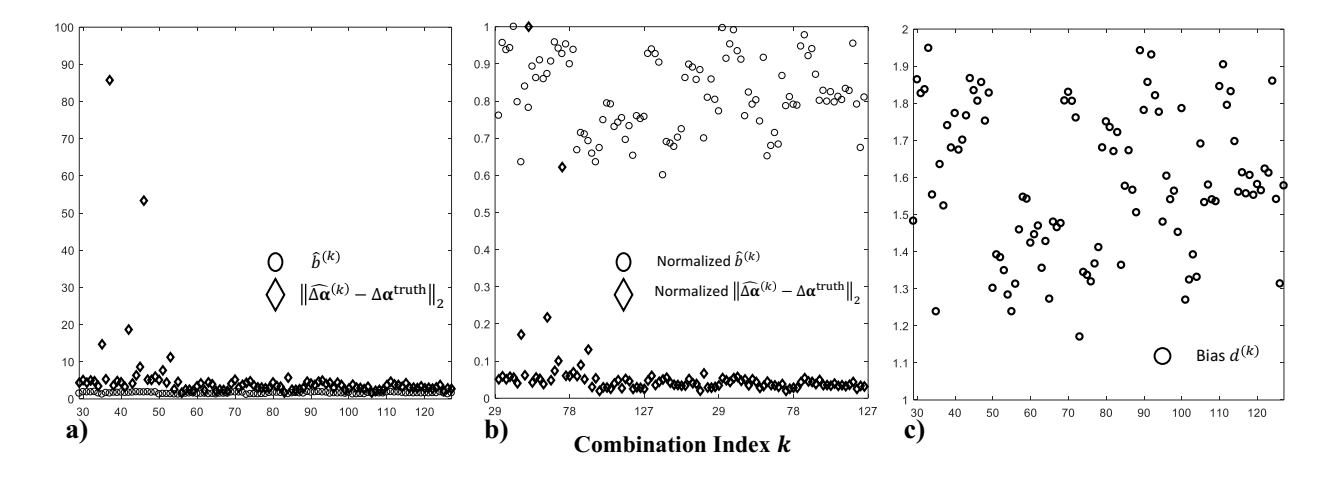


Figure 15. Plots of $\hat{b}^{(k)}$ with $\|\widehat{\Delta\alpha}^{(k)} - \Delta\alpha^{\text{truth}}\|_2$ for k = 29, 30, ..., 127 with severe damage

Figure 15(a) is similar to Figure 5 or 8 showing the comparison between $\hat{b}^{(k)}$ and $\|\widehat{\Delta\alpha}^{(k)} - \Delta\alpha^{\text{truth}}\|_2$. Since they have quite difference scales, the normalized comparison is shown in Figure 15(b). As expected, the two trends are different. For such severe damage scenario, the inaccuracy of the linear approximation causes the overall estimated damage parameters biased from the underlying truth as shown in Figure 15(c). Figure 15(c) presents the bias $d^{(k)}$. It can be seen the average bias for this severe damage case is around 1.7, which is roughly 17 times large than the bias shown in Figure 2. In other words, the estimation of damages can be extremely biased for severe damage scenario.

It is worth to point out that it is more important to estimate mild damage conditions in practice. Severe damages not only reduce natural frequencies significantly, but also cause visible changes in structures. However, mild damages can be hidden from simple visual inspection. Thus, it is more important to identify mild damages accurately for preventive repair or correction.

For practice implementation of the proposed methods, it is suggested to adopt the model updating first to establish high fidelity FE model [19,20]. In practice, model updating can help to correct model parameters in the FEM (e.g. M and K) due to measurement noise or model inadequacy. For a complicated structural system or FEM with thousands of elements, the concerns of implementing the proposed methods and possible solutions are: i) Achieve a reasonable sparse solution from thousands of elements. In general, this is a large p (number of unknows) and small n (number of equations) problem. One possible solution to achieve a reasonable sparsity is to increase the penalty level. For example, the value -0.05 in the majority voting process of the proposed method can be further reduced (e.g. -0.1) to allow more elements to be treated as healthy in the following iterations. Similarly, it is also reasonable to adjust the 95% level (e.g. reduce to 90%) to make the proposed method flexible for a complicated structure. In the proposed method, we choose -0.05 and 95% by the general guidelines from the mechanical engineering and statistics. Indeed, these values are tuning parameters can be adjusted to meet the practice. ii) the accuracy of the linear approximation to describe the dynamics of a system. The proposed method is based on the linear approximation of the structural system. Once the linear approximation is not proper to describe the dynamics of the system, the performance of the proposed method may get hurt (e.g.,

as shown in Figure 13 and 14). In general, the proposed method performs well for mild damages, where the linear approximation preserves high accuracy.

7. Conclusion

In this paper, we propose a natural frequency selection algorithm to reduce the bias in the estimation of damage parameters using linear approximation under mild damage scenarios. The selected combination of natural frequency has high probability to be the optimal combination which leads to the smallest bias in the estimation among all the possible combinations. The proposed method consists of three algorithms. In the first algorithm, the L_1 - norm regularization with iterative matrix randomization is adopted for estimation of damage parameters followed by a majority voting process. In the second algorithm, the damage locations are identified by sequential updating. The improved estimation L_1 - IMR obtained by the third algorithm helps to choose the best combination of measurements in the third algorithm. The effectiveness of the proposed method is validated through numerical studies. Factors that influence the performance of the method are also discussed.

The proposed algorithm is flexible in dealing with natural frequencies, thus has potential to be extended to the schemes with physical modification, e.g., modification through mass addition or tunable sensing systems. The proposed algorithm can be applied to select measurements among different setups of the structure (i.e., different mass additions or tunable inductances), which may provide a better estimation than combining all available modes from all setups. We will investigate along this direction and report our findings in the near future.

Funding/Acknowledgment

This work is supported by the Air Force Scientific Research Office, grant #FA9550-14-1-0384.

Appendix

Table A-1 Iterative Reweighted L_1 Minimization Algorithm [14]

- 1. Set the iteration count l = 0 and $w_i^{(o)} = 1$, i = 1, 2, ... n2. Solve the weighted L_1 minimization problem:
- $\mathbf{x}^{(l)} = \arg\min_{\mathbf{v}} \mathbf{v} \quad \mathbf{x}_{\mathbf{l}|1},$ 3. Update the weights for i = 1, 2, ... n $w_i^{(l+1)} = \frac{1}{\left|x_i^{(l)} + \delta\right|}$ $\mathbf{x}^{(l)} = \arg\min \left\| \mathbf{W}^{(l)} \mathbf{x} \right\|_1$, subject to $\| \mathbf{y} - \mathbf{A} \mathbf{x} \|_2 \le \epsilon$

$$w_i^{(l+1)} = \frac{1}{\left| x_i^{(l)} + \delta \right|}$$

4. Terminate on convergence or l attains the maximum number. Otherwise, increment l and go to step 2.

References

- [1] Wang, Ying, and Hong Hao. "Damage identification scheme based on compressive sensing." Journal of Computing in Civil Engineering 29, no. 2 (2013): 04014037.
- Cha, P. D., and W. Gu. "Model updating using an incomplete set of experimental modes." [2] Journal of sound and vibration 233, no. 4 (2000): 583-596.
- Nalitolela, N. G., J. E. T. Penny, and M. I. Friswell. "A mass or stiffness addition technique [3] for structural parameter updating." International Journal of Analytical and Experimental Modal Analysis 7, no. 3 (1992): 157-168.
- Jiang, L. J., J. Tang, and K. W. Wang. "An enhanced frequency-shift-based damage [4] identification method using tunable piezoelectric transducer circuitry." Smart materials and structures 15, no. 3 (2006): 799.
- [5] Bao, Zhongping, Suresh Goyal, Liang-Jeng Leu, and Subrata Mukherjee. "The role of beam flexibility and ground contact model in the clattering of deformable beams." TRANSACTIONS-AMERICAN SOCIETY OF **MECHANICAL ENGINEERS** JOURNAL OF DYNAMIC SYSTEMS MEASUREMENT AND CONTROL 126, no. 2 (2004): 421-425.
- [6] Jiang, L. J., J. Tang, and K. W. Wang. "On the tuning of variable piezoelectric transducer circuitry network for structural damage identification." Journal of Sound and Vibration 309, no. 3 (2008): 695-717.
- Wong, C. N., W. D. Zhu, and G. Y. Xu. "On an iterative general-order perturbation method [7] for multiple structural damage detection." Journal of Sound and Vibration 273, no. 1 (2004): 363-386...
- [8] Friswell, Michael, and John E. Mottershead. Finite element model updating in structural dynamics. Vol. 38. Springer Science & Business Media, 1995.
- [9] Lee, Eun-Taik, and Hee-Chang Eun. "Update of corrected stiffness and mass matrices based on measured dynamic modal data." Applied Mathematical Modelling 33.5 (2009): 2274-2281.
- Shuai, Q., K. Zhou, Shiyu Zhou, and J. Tang. "Fault identification using piezoelectric [10] impedance measurement and model-based intelligent inference with pre-screening." Smart Materials and Structures 26, no. 4 (2017): 045007.

- [11] Li, Jun, and S. S. Law. "Substructural damage detection with incomplete information of the structure." Journal of applied mechanics 79.4 (2012): 041003.
- [12] Abdalla, M. O., K. M. Grigoriadis, and D. C. Zimmerman. "Structural damage detection using linear matrix inequality methods." Journal of Vibration and Acoustics 122.4 (2000): 448-455.
- [13] Sprent, P. "A generalized least-squares approach to linear functional relationships." Journal of the Royal Statistical Society. Series B (Methodological) (1966): 278-297.
- [14] Chen, Su Huan, Cheng Huang, and Zongjie Cao. "Structural modal reanalysis of topological modifications." Shock and Vibration 7.1 (2000): 15-21.
- [15] Chen, S. H., X. W. Yang, and H. D. Lian. "Comparison of several eigenvalue reanalysis methods for modified structures." Structural and Multidisciplinary optimization 20.4 (2000): 253-259.
- [16] Padil, Khairul H., Norhisham Bakhary, and Hong Hao. "The use of a non-probabilistic artificial neural network to consider uncertainties in vibration-based-damage detection." Mechanical Systems and Signal Processing 83 (2017): 194-209.
- [17] Chondros, T. G., and A. D. Dimarogonas. "Vibration of a cracked cantilever beam." Journal of vibration and acoustics 120.3 (1998): 742-746.
- [18] Koh, Kwangmoo, Seung-Jean Kim, and Stephen Boyd. "An interior-point method for large-scale 11-regularized logistic regression." Journal of Machine learning research 8, no. Jul (2007): 1519-1555..
- [19] Candes, Emmanuel J., Michael B. Wakin, and Stephen P. Boyd. "Enhancing sparsity by reweighted & 1 minimization." Journal of Fourier analysis and applications 14, no. 5 (2008): 877-905.
- [20] Adams, R. D., P. Cawley, C. J. Pye, and B. J. Stone. "A vibration technique for non-destructively assessing the integrity of structures." Journal of Mechanical Engineering Science 20, no. 2 (1978): 93-100.
- [21] Kariya, Takeaki, and Hiroshi Kurata. Generalized least squares. John Wiley & Sons, 2004.
- [22] Westfall, Peter H., and S. Stanley Young. Resampling-based multiple testing: Examples and methods for p-value adjustment. Vol. 279. John Wiley & Sons, 1993.
- [23] Mei, T. X., and H. Li. "Control design for the active stabilization of rail wheelsets." Journal of Dynamic Systems, Measurement, and Control 130, no. 1 (2008): 011002.
- [24] Melbourne, Clive, ed. Arch Bridges: Proceedings of the First International Conference on Arch Bridges Held at Bolton, UK on 3-6 September 1995. Thomas Telford, 1995.
- [25] Liu, Y., Shuai, Q., Zhou, S., & Tang, J. (2017). Prognosis of structural damage growth via integration of physical model prediction and bayesian estimation. IEEE T. Reliab., vol. PP, (99), 1-12.

Figure Captions List

- Figure 1. The fixed-free beam for the simulation. There are total 20 elements in the beam.
- Figure 2. The bias of the estimated damages for different combinations of natural frequencies
- Figure 3. Damage parameter histogram of 20 elements with Algorithm 1. True damages of each element are labeled using dash lines.
- Figure 4. Damage parameter histogram of 20 elements after Algorithm 2. True damages of each element are labeled using dashed lines
- Figure 5. Plots of $\hat{b}^{(k)}$ and $d^{(k)}$ for k = 8, 9, ..., 127.
- Figure 6. Comparison of damage parameter estimation using different approaches.
- Figure 7. Damage parameter histogram of 20 elements after Algorithm 2. True damages of each element are labeled using dash lines
- Figure 8. Plots of $\hat{b}^{(k)}$ and the $\|\widehat{\Delta \alpha}^{(k)} \Delta \alpha^{\text{truth}}\|_2$ for k = 29, 30, ..., 127.
- Figure 9. Comparison of damage parameter estimation using different approaches
- Figure 10. Accuracy of damage location identification by Algorithm 2 under random noise scenarios.
- Figure 11. $\widehat{\Delta \alpha}$ for each iteration q by Algorithm 2. The x-axis is 200 elements and the y-axis is $\widehat{\Delta \alpha}$. The dashed lines are the underlying damage for elements 40 and 170.
- Figure 12. A small mass is attached on the middle of the beam to simulate the stiffness reduction with an accelerometer located near one end of the beam.
- Figure 13. Accuracy of linear approximation in natural frequencies
- Figure 14. Damage parameter histogram of 20 elements after Algorithm 2. True damages of each element are labeled using dashed lines
- Figure 15. Plots of $\hat{b}^{(k)}$ with $\|\widehat{\Delta \alpha}^{(k)} \Delta \alpha^{\text{truth}}\|_2$ for k = 29, 30, ..., 127 with severe damage

Table Caption List

- Table 1. Algorithm 1: Iterative Random Matrix Multiplication and Majority Voting
- Table 2. Algorithm 2: Damage Location Identification Algorithm
- Table 3. Algorithm 3: Natural Frequency Selection Algorithm for Bias Reduction
- Table 4. Parameters of the Beam Structure
- Table 5. The First Seven Natural Frequencies (HZ) (n.f.)
- Table 6. Performance of the Proposed Algorithm in Different Damage Scenarios
- Table 7. Parameters of the Real Beam Structure
- Table 8. Natural Frequencies (Hz) Before and After Mass Added
- Table A-1 Iterative Reweighted L_1 Minimization Algorithm [15]